ELSEVIER

Journal of Hydrology 242 (2001) 137–155

Journal of Hydrology

www.elsevier.com/locate/jhydrol

A stochastic approach to short-term rainfall prediction using a physically based conceptual rainfall model

S. Sugimoto[a,*], E. Nakakita[b,1], S. Ikebuchi[c,2]

[a]*Environmental Science Department, Central Research Institute of Electric Power Industry, Abiko, Chiba 270-1194, Japan*
[b]*Department of Global Environment Engineering, Kyoto University, Yoshida-honmachi, Sakyo-ku, Kyoto 606-8501, Japan*
[c]*Water Resources Research Center, Disaster Prevention Research Institute, Kyoto University, Uji, Kyoto 611-0011, Japan*

Received 13 October 1999; revised 13 October 2000; accepted 23 October 2000

Abstract

An improved method for short-term rainfall prediction is presented. A previously proposed deterministic rainfall prediction method for real-time hydrologic applications is extended to a stochastic method. This method mainly consists of a physically based conceptual rainfall model that includes water balance and thermodynamics. The important element in this method is the translation of radar data to the model parameter of the conceptual model, which is incorporated into the numerical scheme of the mesoscale model. The extended Kalman filter is used as a state estimator to update the model parameter of the conceptual model with new radar data and with forecasts from a numerical weather prediction model. The performance of the stochastic method is examined for a radar observation area that includes a mountainous region with a rainfall event that occurred along a front. The stochastic method performed better than the deterministic method. © 2001 Elsevier Science B.V. All rights reserved.

Keywords: Rainfall prediction; Radar; Conceptual model; Stochastic processes; Kalman filter

1. Introduction

Quantitative rainfall prediction provides valuable information for preventing or mitigating flash flooding. Predicting rainfall hours in advance, corresponding to the time lag of basin response, is a particularly important to avoid flood danger. This demonstrates the great importance of a reliable short-term rainfall prediction method.

The rainfall prediction method used in this work is a physically based, short-term rainfall prediction method developed by Nakakita et al. (1996). The method utilizes three-dimensional information routinely obtained from three sources: a conventional volume-scanning C-band radar, ground station data from the Automated Meteorological Data Acquisition System (AMeDAS), and grid point values (GPV) from a numerical weather prediction (NWP) model called the Japan Spectral Model (JSM). AMeDAS and JSM are managed and developed by the Japan Meteorological Agency (JMA). This method does not use the GPV of rainfall because the horizontal and temporal resolution of GPV data is sparse compared to that of radar data. The additional utilization of radar information allows this method to predict the GPV subgrid variability of rainfall.

* Corresponding author. Tel.: +81-471-82-1181; fax: +81-471-83-2966.

E-mail addresses: soichiro@criepi.denken.or.jp (S. Sugimoto), nakakita@info.gee.kyoto-u.ac.jp (E. Nakakita), chief@wrcs.dpri.kyoto-u.ac.jp (S. Ikebuchi).

[1] Fax: +81-757-53-5109.

[2] Fax: +81-774-32-3093.

0022-1694/01/$ - see front matter © 2001 Elsevier Science B.V. All rights reserved.
PII: S0022-1694(00)00390-5

Nomenclature

h	terrain height (m)
L	latent heat of condensation (J/kg)
m_l	mixing ratio of precipitation particles (kg/kg)
m_v	mixing ratio of water vapor (kg/kg)
m_s	saturation mixing ratio (kg/kg)
Q	conversion rate of water vapor (CRWV) (kg/(m^3 s))
r	rainfall intensity (m/s)
R_d	individual gas constant for dry air (287 J/(kg K))
R_v	gas constant for water vapor (461 J/(kg K))
(u,v)	horizontal wind velocity (m/s)
w	vertical wind velocity (m/s)
W_t	relative fall velocity of precipitation particles (m/s)
z	vertical coordinate in Cartesian coordinates (m)
s	vertical coordinate in the σ-coordinate system
α	model parameter
p	air pressure (hPa)
ρ	air density (kg/m^3)
ρ_w	density of liquid water (kg/m^3)
θ	potential temperature (K)
T	air temperature (K)
(U,V)	advection vector of the model parameter (m/s)

The previous prediction method, however, was deterministic in the primary stages of study. In the present method, the conversion rate of water vapor (CRWV) is retrieved from radar information using the conservation equation of liquid water content as proposed by Nakakita et al. (1990, 1991, 1996). Then the model parameter of the conceptual rainfall model proposed by Nakakita et al. (1990, 1991, 1996, 1998a), which defines the amount of water vapor converted to liquid water, can be identified using principles of water balance and thermodynamics. Rainfall is simulated and predicted by extrapolating the model parameter along the advection vector calculated by Takasao and Shiiba (1985) assuming simple advection. This method extrapolates the model parameter, not the pattern of movement of the horizontal rainfall distribution.

The conceptual rainfall model assumes that an interaction between the movement of the model parameter and the water vapor field under the influence of topography can predict heavy rainfall in mountainous regions. As a result of using the deterministic method, a radically changing rainfall distribution that is influenced by complex terrain can be predicted qualitatively. Features such as generation, growth, decay, and persistence of rainfall areas cannot be predicted by any method that is based on an extrapolation of rainfall distribution itself. At present, the deterministic method is used at the Ministry of Construction of Japan and our research has entered upon the second phase of the feasibility study.

The main objective of this work is to introduce a stochastic concept into the deterministic method proposed by Nakakita et al. (1996). This extended method provides a means of considering uncertainties due to model formulation errors and observation errors. To take uncertainties into account, this work formulates the conceptual rainfall model in state–space mathematical form suitable for the design of a state estimator such as the extended Kalman filter. In general, the algorithm that uses the extended Kalman filter allows automatic and recursive updates of the model states from routinely available observations. In this work, the model parameter of the conceptual rainfall model is updated by using the radar reflectivity to estimate the mixing ratio of precipitation particles once per hour.

Previous models that forecast precipitation using stochastic–dynamical methods have performed well. Georgakakos and Bras (1984a,b) developed a spatially lumped model using microphysical parameterizations for short-term prediction of rainfall on hydrologic scales. Lee and Georgakakos (1990) extended the formulation to two dimensions. These models include the following: raingauge data, theory-based parameterization of water vapor condensation, precipitation, evaporation of precipitation hydrometeors, and a state estimator for real-time updating of liquid water equivalent average mass condensed in a cloud column from local rainfall data. Lee and Georgakakos (1996) introduced an additional dynamics equation for the advection of convective regions by estimating the degree of updraft strength from convective available potential energy (CAPE). Consequently, it became possible to produce higher-resolution precipitation forecasts, even if the model performance is sensitive to the performance of the NWP model that is used. The first three models also showed that stochastic models perform better than deterministic ones. It was found that rainfall rates transformed from reflectivity factors greatly improves the model performance. Georgakakos and Krajewski (1991) also studied the value of radar data in rainfall forecasting.

The other pertinent works to stochastic–dynamical modeling and forecasting can be found in French and Krajewski (1994) and French et al. (1994). They used microphysical parameterizations similar to Georgakakos and Bras (1984a) and rainfall dynamics based on Seo and Smith (1992), which considered mass balancing of vertically integrated liquid water content (VIL) estimated from radar reflectivity. It is important that they developed a spatially distributed model that can utilize radar data. In their stochastic framework, the system state is a vector of VIL that defines the evolution of the system. The results from an application of their stochastic model to the Plains region of the United States demonstrated better performance than persistence or advection methods. Andrieu et al. (1996) presented an approach for incorporating orographic rainfall enhancement into the model of French and Krajewski (1994): the moisture source parameterization was modified to explicitly account for the mesoscale rain system and orographic influences. The results showed that the source term representing the moisture input to the atmospheric column is important, which is significantly influenced by the estimated mesoscale updraft velocity.

It should be emphasized that our approach is similar to the aforementioned studies in that we use a conceptual rainfall model based on simplified thermodynamics and microphysics. Nakakita et al. (1996) classified operational short-term rainfall prediction methods into three categories: (1) those that extrapolate the movement pattern of a horizontal rainfall distribution (Wilk and Gray, 1970; Austin and Bellon, 1974; Bellon and Austin, 1978; Takasao and Shiiba, 1985; Bellon and Zawadzki, 1994); (2) those that use the principles of water balance and thermodynamics with a conceptual rainfall model; and (3) those that either use the full set of conservation equations at the mesoscale (Pielke, 1984) or use a method that reduces the grid size of NWP (Ninomiya et al., 1984). Georgakakos and Hudlow (1984), Georgakakos and Kavvas (1987), and Browning and Collier (1989) reviewed operational rainfall prediction procedures in detail.

The third category of method seems to be most accurate, but we believe that such methods would be difficult to implement for a real-time operational prediction method because of three difficulties. First, large computational resources are required. Second, data input and surface boundary information with sufficiently high-resolution in space and time are not available from routine observations and this method tends to amplify small initial perturbations in the atmospheric fields. Third, sufficiently accurate cloud model parameterizations have not yet been established.

On the other hand, the first category of method is used in nowcasting, but the effect of topography cannot be incorporated physically into a rainfall model. So, it appears that this approach works well for widespread rainfall over lowland areas, but not for convective and orographic rainfall. Conversely, Oriville (1965), Colton (1976), Bradlay (1984), and Yoshizaki and Ogura (1988) could simulate orographic precipitation processes. These studies suggest that some features of rainfall phenomena are associated with orographic influences. Therefore, we propose a stochastic rainfall prediction method by extending the prediction method proposed by Nakakita et al. (1996) belonging to the second category.

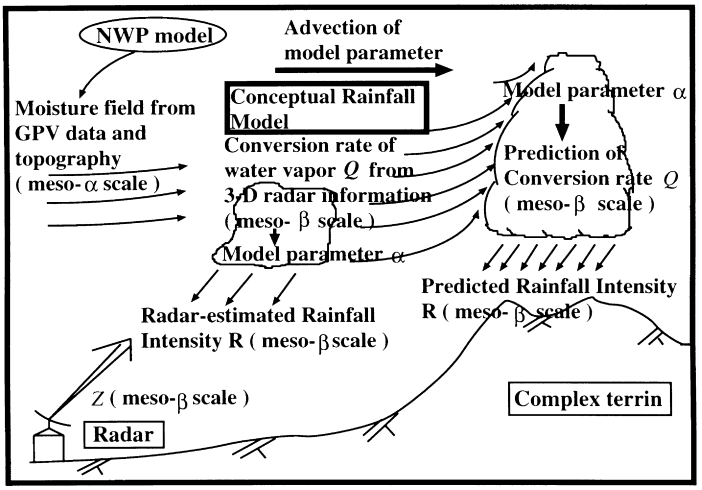

Fig. 1. Schematic representation of the rainfall prediction method.

This paper is organized in the following manner. Section 2 outlines the deterministic method developed by Nakakita et al. (1996). In Sections 3 and 4, an extension to a stochastic method is proposed and applied. These sections include results and discussion. We close with Section 5 in which conclusions and recommended topics for future study are discussed.

2. Outline of the deterministic physically based rainfall prediction method

The basic equations used in the physically based method are sets of partial differential equations for conservation of liquid water, heat, and water vapor at the mesoscale, and an equation for estimating the rainfall intensity. These equations are written as (following the notation of Nakakita et al. (1996)):

$$\frac{\partial m_l}{\partial t} + u\frac{\partial m_l}{\partial x} + v\frac{\partial m_l}{\partial y} + w\frac{\partial m_l}{\partial z} = \frac{Q}{\rho} + \frac{\rho_w}{\rho}\frac{\partial r}{\partial z}, \quad (1)$$

$$\frac{\partial \theta}{\partial t} + u\frac{\partial \theta}{\partial x} + v\frac{\partial \theta}{\partial y} + w\frac{\partial \theta}{\partial z} = \frac{LQ}{\rho C_p}\left(\frac{1000}{p}\right)^{R_d/C_p}, \quad (2)$$

$$\frac{\partial m_v}{\partial t} + u\frac{\partial m_v}{\partial x} + v\frac{\partial m_v}{\partial y} + w\frac{\partial m_v}{\partial z} = -\frac{Q}{\rho}, \quad (3)$$

$$r = \frac{\rho}{\rho_w} W_t m_l, \quad (4)$$

where x, y, and z define Cartesian coordinates in the two horizontal directions and the vertical, respectively; u, v, and w are velocities of the air in the x-, y-, and z-Cartesian directions in m/s; m_l is the mixing ratio of precipitation particles in kg/kg; m_v is the mixing ratio of water vapor in kg/kg; θ is the potential temperature in K; Q is the conversion rate of water vapor (CRWV) in kg/m^3/s; r is the rainfall intensity in m/s; L is the latent heat of vaporization in J/kg; C_p is the specific heat at constant pressure in J/K/kg; R_d is the individual gas constant for dry air in J/K/kg; p is the air pressure in hectopascals; W_t is the relative fall velocity of water particles in m/s; and ρ and ρ_w are the density of air and liquid water in kg/m^3, respectively. The CRWV is defined as the amount of water vapor converted to precipitation particles per unit time and unit volume. There is no provision for cloud particles because they cannot be detected by conventional radar. The terminal velocity W_t is from Ogura and Takahashi (1971); it relates the water content of the air to the mean volume-weighted terminal velocity.

These basic equations are transformed from the Cartesian coordinates (x,y,z) into a terrain-following coordinate system (x,y,s) according to Colton (1976). The transformation can be written as

$$s = \frac{z - h(x,y)}{H - h(x,y)}, \quad (5)$$

where H is the elevation of the top grid point in the model (= 11 000 m) and $h(x,y)$ is the terrain elevation.

GPV data with meso-α-scale resolution are used to estimate the three-dimensional wind vector (u,v,w), the air temperature, air pressure, and water vapor field (Nakakita et al., 1996). The estimated wind and pressure fields are assumed to be constant during the prediction procedure and are used as initial values. Using Marshall and Palmer's (1948) drop size distribution for rain and Gunn and Marshall's (1958) for snow, the past and current three-dimensional distributions of the rainfall intensity r and the mixing ratio of precipitation particles m_l are estimated from the three-dimensional distribution of the radar reflectivity factor (Nakakita et al., 1990, 1991, 1996).

A schematic of the rainfall prediction method developed by Nakakita et al. (1996) is given in Fig. 1. The method involves several steps that are presented in more detail in Nakakita et al. (1996). Here, an important part of their method is estimating the three-dimensional distribution of the CRWV Q on the meso-β scale using Eq. (1) based on the retrieval method proposed by Nakakita et al. (1990, 1991, 1996). Additionally, the three-dimensional distributions of θ and m_v at the scale of Q are retrieved with identifying the model parameter using the conservation equations and both the CRWV and the wind-vector distributions.

The CRWV can be estimated using Eq. (1) because (u,v,w), m_l, and r have been already estimated. In other words, the past and current CRWV distributions can be estimated using the past and current radar-reflectivity distributions. Therefore, the CRWV can be retrieved only in the domain of existing radar echo. If $Q < 0$, precipitation particles must evaporate.

The method used to retrieve θ and m_v and to identify the model parameter will be described later with the integration procedure of the governing equations (1)–(3).

2.1. Original concept of rainfall model

We outline here the rainfall model originally proposed by Nakakita et al. (1990, 1991, 1996, 1998a). It consists of two important steps.

In one of the steps, θ and m_v are retrieved in a warm-up run for 2 h. The warm-up run was based on the water balance and thermodynamics described in the Appendix A and on fixed known distributions of Q, p, and (u,v,w). For this warm-up run, the distributions of θ and m_v already estimated on the meso-α scale from GPV data are used as initial distributions. In this stage, δm in Eq. (A2) is not estimated by Eqs. (A1) and (A2), but computed using Q:

$$\delta m = \Delta t \frac{Q}{\rho}, \tag{6}$$

where Δt is the temporal increment of the finite difference: This is because the model parameter is not yet identified whereas Eqs. (A1) and (A2) are only applicable after the model parameter is identified. The purpose of these retrievals is to reduce the difference between the spatial resolutions of θ and m_v (i.e. the resolution of GPV data) and that of Q (i.e. the resolution of radar information).

If the distributions of θ and m_v are retrieved, the model parameter is identified so that the index of efficiency of converting water vapor to liquid water precipitation in the precipitation field of interest can be estimated. The model parameter introduced in the conceptual rainfall model is defined as follows. The modified saturation mixing ratio $\overline{m_s'}$ is given by

$$\overline{m_s'} = (1 - \alpha) m_s, \tag{7}$$

where α is the model parameter and m_s the saturation mixing ratio. The following empirical formula (Pielke, 1984) was used for m_s:

$$m_s = \frac{3.8}{p} \exp\left[\frac{17.3(T(\theta,p) - 273.2)}{T(\theta,p) - 35.9}\right], \tag{8}$$

where the notation $T(\theta,p)$ indicates that T can be calculated according to the definition of potential temperature θ.

In this definition, the difference between m_s and $\overline{m_s'}$ indicates the degree of shortage of vertical water vapor flux brought on by the meso-α field. This shortage is because the moisture field used cannot cause strong convection at the scale of meso-β; this definition serves to make up this shortage. As is mentioned in Nakakita et al. (1996), this conceptual rainfall model bridges the gap between radar data and NWP model scales. This definition implies that heavy rainfall is prone to occur where the model parameter is large.

It can be seen from Eqs. (6), (A1) and (A2) that the spatial and temporal variation of the three-dimensional CRWV Q is closely related with that of the model parameter α. Substituting Eqs. (6) and (A1)

into Eq. (A2) yields

$$\alpha = 1 - \left[\frac{1}{m_s^*} \left(m_v^* - \Delta t \frac{Q}{\rho} \right) \right] \Big/ \left[1 + \Delta t \frac{Q}{\rho} \frac{L^2}{C_p R_v} \frac{1}{\theta^{*2}} \left(\frac{1000}{p} \right)^{2R_d/C_p} \right], \quad (9)$$

where the superscript * denotes the intermediate values retrieved after the warm-up run. The model parameter α can be estimated only in the domain where radar echo exists. These identified and retrieved distributions of α, θ, and m_v are used as initial conditions for the rainfall prediction. A rainfall field itself should have orographic influences. However, α is not likely to be influenced by the complexity of terrain because this model represents orographic effects on a rainfall distribution. Thus, we assume that the structure of the model parameter does not change during its movement across the radar observation area in the prediction procedure.

2.2. Prediction procedure

The three-dimensional distributions of θ, m_v, Q, and m_l are integrated as described in the Appendix A. In the prediction procedure, the three-dimensional distribution of α is calculated by simple horizontal advection of the identified distribution of α. This assumption is used because α is not likely to be affected by complex terrain. That is

$$\frac{\partial \alpha(x,y,z)}{\partial t} + U \frac{\partial \alpha(x,y,z)}{\partial x} + V \frac{\partial \alpha(x,y,z)}{\partial y} = 0. \quad (10)$$

An advection vector (U,V) of the model parameter is determined using an advection model proposed by Takasao and Shiiba (1985). The use of (U,V) instead of (u,v) that is forecasted by NWP is intended for real-time estimation of the wave velocity that drives the entire rainfall field.

Then, after basic equations (1)–(4) are integrated simultaneously, the three-dimensional distribution of rainfall intensity r can be predicted from Eq. (4) as a final output. This output is then transformed into Cartesian coordinates. Model limitations due to assumptions and simplifications are discussed by Nakakita et al. (1996).

3. Stochastic framework of rainfall prediction procedure

Predictions of rainfall intensity are expected to contain errors because several simplifications are made to the model physics for the purpose of practical use. It is thus imperative that new observations (e.g. radar data) or forecasts (e.g. GPV data) are used in real time as they become available to update model state variables and also that the method is capable of stochastic prediction. A state estimator allows stochastic prediction and recursive updating of state variables from current rainfall observations.

The most common optimal filtering technique is that developed by Kalman (1960) for estimating the state of a linear system. The Kalman filter defines a framework for recursive solution to an optimization problem and the processing of measurement data: it includes uncertainties in both model and observation. For a nonlinear system, one practical method is to apply the Kalman filter to the system linearized by the Taylor expansion. This method is called the extended Kalman filter.

The adjoint method (LeDimet and Talagrand, 1986) appears to be considerably less expensive computationally than the Kalman filter. The Kalman filter is different from the adjoint technique in that the adjoint method does not account for model errors: model dynamics are assumed to accurately represent atmospheric dynamics. In this section, a state estimator using the extended Kalman filter is designed and implemented to achieve the goal of providing hydrologically useful rainfall predictions.

3.1. Algorithm using the extended Kalman filter

We briefly review the theory of the discrete extended Kalman filter. For more detail, see Anderson and Moore (1979), Gelb (1974), and Jazwinski (1970).

Suppose the evolution of the true system being modelled is described by

$$\mathbf{w}_k^t = \mathbf{A}_{k,k-1}\mathbf{w}_{k-1}^t + \mathbf{b}_k^t \qquad (k = 1, 2, \ldots), \quad (11)$$

where $\mathbf{w}_k^t$ is the n-vector true state at time t_k, $\mathbf{A}_{k,k-1}$ is the $n \times n$ state transition matrix, and the n-vector $\mathbf{b}_k^t$ is a random vector that is called the model error. In a finite-difference model, n is the number of grid points

times the number of prognostic variables. The model error is assumed to be white with no time structure representing imperfections in the prediction method and with mean zero and covariance matrix $\mathbf{Q}_k$:

$$E[\mathbf{b}_k^{\mathrm{t}}] = 0, \tag{12}$$

and

$$E[\mathbf{b}_k^{\mathrm{t}}(\mathbf{b}_{k'}^{\mathrm{t}})^{\mathrm{T}}] = \begin{cases} \mathbf{Q}_k & \text{for } k = k' \\ 0 & \text{otherwise} \end{cases}, \tag{13}$$

where $E[\,]$ denotes the expectation operator and superscript T denotes the transpose of matrix or vector quantities.

The objective of filtering is to estimate the true system state $\mathbf{w}_k^{\mathrm{t}}$ utilizing the new observations. Suppose that the prediction model is given by

$$\begin{aligned} \mathbf{w}_k^{\mathrm{f}} &= \mathbf{A}_{k,k-l}\mathbf{w}_{k-l}^{\mathrm{a}} \qquad \text{for } k \text{ a multiple of } l \\ &= \mathbf{A}_{k,k-1}\mathbf{A}_{k-1,k-2}\cdots\mathbf{A}_{k-l+1,k-l}\mathbf{w}_{k-l}^{\mathrm{a}}, \end{aligned} \tag{14}$$

where $\mathbf{w}_{k-l}^{\mathrm{a}}$ denotes the a posteriori updated state valid at the time t_{k-l} based on the a priori information available at time t_{k-l} and $\mathbf{w}_k^{\mathrm{f}}$ is the forecasted state at the time t_k. The filtering algorithm provides the error covariances of analysis and forecast, and the updated state vector:

$$\mathbf{P}_k^{\mathrm{f,a}} = \mathbf{E}[(\mathbf{w}_k^{\mathrm{f,a}} - \mathbf{w}_k^{\mathrm{t}})(\mathbf{w}_k^{\mathrm{f,a}} - \mathbf{w}_k^{\mathrm{t}})^{\mathrm{T}}], \tag{15}$$

where $\mathbf{P}_k^{\mathrm{f}}$ is defined as the forecast error covariance and $\mathbf{P}_k^{\mathrm{a}}$ as the analysis error covariance.

The propagation equation follows from the above assumptions:

$$\mathbf{P}_k^{\mathrm{f}} = \mathbf{A}_{k,k-l}\mathbf{P}_{k-l}^{\mathrm{a}}\mathbf{A}_{k,k-l}^{\mathrm{T}} + \sum_{j=0}^{l-1}\mathbf{A}_{k,k-j}\mathbf{Q}_{k-j}\mathbf{A}_{k,k-j}^{\mathrm{T}}. \tag{16}$$

We assume further that observations $\mathbf{w}_k^{\mathrm{o}}$ are a nonlinear combination of elements of the true state vector $\mathbf{w}_k^{\mathrm{t}}$:

$$\mathbf{w}_k^{\mathrm{o}} = h_k(\mathbf{w}_k^{\mathrm{t}}) + \mathbf{b}_k^{\mathrm{o}}, \tag{17}$$

where $\mathbf{w}_k^{\mathrm{o}}$ is the p-vector of observations at time t_k. $h_k(\mathbf{w}_k)$ defines the observational scheme and depends nonlinearly upon both index k and the state at each sampling time. The observation error $\mathbf{b}_k^{\mathrm{o}}$ is assumed to be white with mean zero and covariance matrix $\mathbf{R}_k$ and to be uncorrelated with the model error:

$$E[\mathbf{b}_k^{\mathrm{o}}] = 0, \tag{18}$$

and

$$E[\mathbf{b}_k^{\mathrm{o}}(\mathbf{b}_{k'}^{\mathrm{o}})^{\mathrm{T}}] = \begin{cases} \mathbf{R}_k & \text{for } k = k' \\ 0 & \text{otherwise} \end{cases}. \tag{19}$$

The update process combines the latest estimate of the state with repetitive observations. Given the new observation at time t_k, we expand $h_k(\mathbf{w}_k^{\mathrm{t}})$ in a Taylor series about the current estimate of the state vector $\mathbf{w}_k^{\mathrm{f}}$:

$$h_k(\mathbf{w}_k^{\mathrm{t}}) = h_k(\mathbf{w}_k^{\mathrm{f}}) + \mathbf{H}_k(\mathbf{w}_k^{\mathrm{t}} - \mathbf{w}_k^{\mathrm{f}}) + \cdots, \tag{20}$$

where

$$\mathbf{H}_k = \left.\frac{\partial h_k(\mathbf{w})}{\partial \mathbf{w}}\right|_{\mathbf{w}=\mathbf{w}_k^{\mathrm{f}}}. \tag{21}$$

Truncating the above series after the first two terms, the extended Kalman filter update equations are formulated similar to the conventional Kalman filter:

$$\mathbf{w}_k^{\mathrm{a}} = \mathbf{w}_k^{\mathrm{f}} + \mathbf{K}_k(\mathbf{w}_k^{\mathrm{o}} - \mathbf{H}_k\mathbf{w}_k^{\mathrm{f}}), \tag{22}$$

$$\mathbf{K}_k = \mathbf{P}_k^{\mathrm{f}}\mathbf{H}_k^{\mathrm{T}}(\mathbf{H}_k\mathbf{P}_k^{\mathrm{f}}\mathbf{H}_k^{\mathrm{T}} + \mathbf{R}_k)^{-1}, \tag{23}$$

$$\mathbf{P}_k^{\mathrm{a}} = (\mathbf{I} - \mathbf{K}_k\mathbf{H}_k)\mathbf{P}_k^{\mathrm{f}}, \tag{24}$$

where the last factor in Eq. (23) is the matrix inverse of the quantity in parenthesis. $\mathbf{K}_k$ is called the Kalman gain matrix; it is the weight matrix applied to the observed-minus-forecast residual in Eq. (22) to yield the analysis field $\mathbf{w}_k^{\mathrm{a}}$. The extended Kalman filter is defined by Eqs. (14), (16), and (22)–(24). The propagation process and the update process are the intensive algorithms of the Kalman filter. Given the initial condition for Eqs. (14) and (16), the state vector can be updated recursively as new observations of the output of the system become available.

The extended Kalman filter is different from the conventional Kalman filter as follows: the gain matrix $\mathbf{K}_k$ depends upon the estimate $\mathbf{w}_k^{\mathrm{f}}$. Hence, $\mathbf{K}_k$ cannot be computed before observations are collected, so it must be computed in real time. The estimation error covariance $\mathbf{P}_k^{\mathrm{a}}$ also depends upon the trajectory of the state variables.

Many other appropriate nonlinear filters are based on using more terms in the Taylor series expansion or

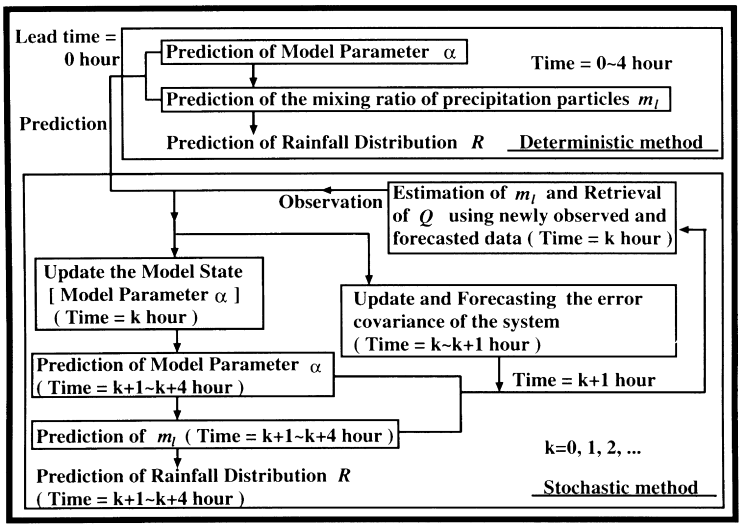

Fig. 2. Flowchart showing the stochastic framework.

iterating the extended Kalman filter in various ways. Though more complicated filter equations for nonlinear problems are known, their solutions require closure or other assumptions (Jazwinski, 1970). For this reason, the extended Kalman filter is useful and is one of the first methods to be attempted for most practical problems.

3.2. Outline of the filtering procedure

Fig. 2 shows a flow chart of data processing in a stochastic framework including the prediction procedure of the deterministic method. The state variable is the model parameter α of the conceptual rainfall model and the mixing ratio of precipitation particles m_l is used recursively in this framework. As mentioned in the previous section, α defines the amount of water vapor converted to liquid water and it greatly affects the prediction. Therefore, α can be regarded as an index that defines the evolution of the system. On the other hand, as can be seen from Eqs. (A2) and (A5), α is sensitive to the temporal variation of m_l; furthermore, m_l is a key variable because rainfall intensity is a function of m_l and the terminal velocity W_t in Eq. (4). In the stochastic framework, the distribution of m_l estimated using radar data is utilized to update α. This is important for reducing the discrepancy between predicted values (i.e. m_v, θ, and m_l) that represent the atmospheric state and the rainfall field observed by a radar. In this framework, prediction errors of α cause prediction errors of m_l.

The state of the system is updated at 1-h intervals from both the distributions of newly estimated m_l and that of α predicted 1 h later; this update is based on α estimated as the initial value 1 h earlier. The stochastic method computes not only the predicted state value but also the covariance matrix of the prediction error in a sequential manner at the same time. In this framework, the rainfall distribution r can be predicted over lead times of 4 h by repeatedly using the updated α as the initial value.

3.3. Mathematical formulation

The filtering equations allow objective, optimal, and recursive updating of the model state (i.e. the model parameter α) from new observations (i.e. the mixing ratio of precipitation particles m_l). In the stochastic framework, the evolution equation of the system state can be formulated in the state–space form:

$$\alpha_k^{f,a} = \mathbf{w}_k^{f,a}, \qquad \alpha_k^{f} = L_{k,k-1}\alpha_k^{a} + \hat{\mathbf{b}}_k, \tag{25}$$

where α_k is the n-vector system state with elements corresponding to the squares of the domain at time t_k. The operator $L_{k,k-l}$ represents advection from time t_{k-l} to time t_k. The stochastic forcing term is assumed

white:

$$E[\hat{\mathbf{b}}_k^{\mathrm{t}}(\hat{\mathbf{b}}_{k'}^{\mathrm{t}})^{\mathrm{T}}] = \begin{cases} \hat{\mathbf{Q}}_k & \text{for } k = k' \\ 0 & \text{otherwise} \end{cases}. \tag{26}$$

Then the error covariance evolution equation corresponding to Eq. (16) is derived as

$$\mathbf{P}_k^{\mathrm{f}} = L_{k,k-l}\mathbf{P}_k^{\mathrm{a}}L_{k,k-l}^{\mathrm{T}} + \hat{\mathbf{Q}}_k. \tag{27}$$

In the conceptual rainfall model, the distribution of α is predicted by a simple advection using Eq. (10), that is, the advection of the model parameter over a time period Δt amounts to a shift in position by ($U\Delta t$,$V\Delta t$):

$$L_{k,k-l} = L, \tag{28}$$

where the operator L calculates the shift ($U{\cdot}l\Delta t$, $V{\cdot}l\Delta t$). Furthermore, the model forcing over a complete prediction cycle is accounted for by taking

$$\hat{\mathbf{Q}}_k = l{\cdot}\mathbf{Q}_k. \tag{29}$$

In this work, the contribution to the evolution of the prediction error covariance will be approximated only as a final step at the end of a prediction cycle. The full propagation equations of the error covariance, represented by Eqs. (13) and (16) in the conventional Kalman filter, are replaced with Eqs. (27) and (29).

Particularly in a nonlinear case, the transition matrix $\mathbf{A}_{k,k-1}$ depends on the state trajectory; hence, it is not clear that additive error forcing should only occur at the prediction model time-step intervals. The expensive computational demand for prediction of the error covariance is reduced by this method. Dee (1990) successfully used such a simple scheme; this had nearly the same advantages of the Kalman filter with a linear one dimensional shallow-water model. The form of $\hat{\mathbf{Q}}_k$ will be discussed later in this section.

Recall the relationship representing the observational scheme. From Eqs. (A1), (A2), and (A5), we find

$$m_{\mathrm{l}}(k) - m_{\mathrm{l}}^*(k) = \frac{m_{\mathrm{v}}^*(k) - (1-\alpha_k^{\mathrm{f}})m_{\mathrm{s}}^*(k)}{1 + (1-\alpha_k^{\mathrm{f}})d_k m_{\mathrm{s}}^*(k)}, \tag{30}$$

with

$$d_k = \frac{1}{\theta^{*2}(k)}\frac{L^2}{C_p R_{\mathrm{v}}}\left(\frac{1000}{p(k)}\right)^{2R_{\mathrm{d}}/C_p}, \tag{31}$$

where those values with k depend on time. In the stochastic framework, $(m_{\mathrm{l}}(k) - m_{\mathrm{l}}^*(k))$ is the observed value because the intermediate value $m_{\mathrm{l}}^*(k)$ is available and $m_{\mathrm{l}}(k)$ is estimated at time t_k. Here, assuming $\mathbf{w}_k^{\mathrm{o}}$ to be the p-vector of $(m_{\mathrm{l}}(k) - m_{\mathrm{l}}^*(k))$, and neglecting second and higher terms in the Taylor expansion of Eq. (30), h_k and $\mathbf{H}_k$ in Eqs. (20) and (21) are determined at each p-grid node in space at time t_k as:

$$h_k = \frac{m_{\mathrm{v}}^*(k) - (1-\alpha_k^{\mathrm{f}})m_{\mathrm{s}}^*(k)}{1 + m_{\mathrm{s}}^*(k)(1-\alpha_k^{\mathrm{f}})d_k}, \tag{32}$$

$$\mathbf{H}_k = \frac{m_{\mathrm{s}}^*(k)(1 + d_k m_{\mathrm{v}}^*(k))}{[1 + m_{\mathrm{s}}^*(k)(1-\alpha_k^{\mathrm{f}})d_k]^2}. \tag{33}$$

We assume that the observation error covariance $\mathbf{R}_k$ is diagonal because observational errors are generally independent. In this work, the observational error at each grid node is proportional to $(m_{\mathrm{l}}(k) - m_{\mathrm{l}}^*(k))$, so the variance $\mathbf{r}_k$, which is a diagonal element of $\mathbf{R}_k$, can be expressed with a coefficient of error σ as

$$\mathbf{r}_k = [(m_{\mathrm{l}}(k) - m_{\mathrm{l}}^*(k))\cdot\sigma]^2. \tag{34}$$

If the newly estimated m_{l} at a grid node is not available at time t_k, the state variable at this grid node cannot be updated. The state remains unchanged from the a priori estimate in this case (i.e. $\mathbf{K}_k = \mathbf{0}$, $\mathbf{P}_k^{\mathrm{a}} = \mathbf{P}_k^{\mathrm{f}}$). On the other hand, if the state $\mathbf{w}_k^{\mathrm{f}}$ before updating is undefined, the update algorithm is as follows:

1. If the newly retrieved CRWV at this grid node is also undefined, the updated state remains undefined.
2. If the newly retrieved CRWV at this grid node is defined, the updated state is obtained from Eq. (9).

Finally, we should check the structure of the covariance matrix $\mathbf{Q}_k$ from a viewpoint of the enormous computational burden due to a very large number of components. Moreover, a discussion on the choice of $\mathbf{Q}_k$ form is required. The cost of computing the covariance matrix has prevented widespread use of the Kalman filter (Bennett and Budgell, 1987). Brute-force calculation of the forecast error covariance is not feasible. Nevertheless, the choice of the model error covariance matrix exerts considerable influence upon the forecast error covariance matrix (Phillips, 1982).

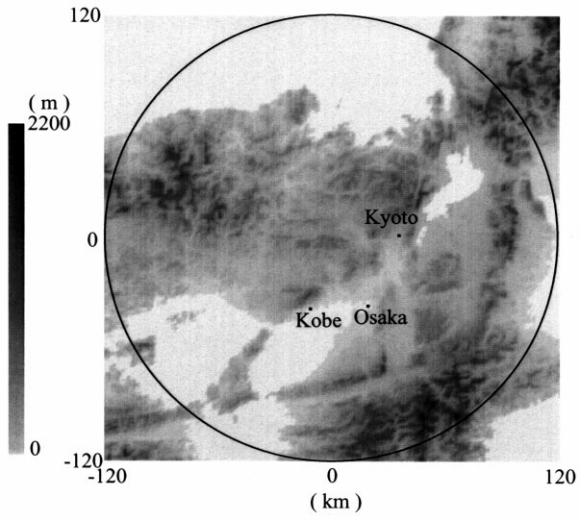

Fig. 3. The radar observation area. The circle indicates the range of the radar observation.

For strictly linear dynamics, Cohn and Parrish (1991) theoretically and numerically demonstrated the influences of the form of $\mathbf{Q}_k$ by assuming model errors to consist of uncorrelated slow modes. The modal expansion coefficients of the model error field can be introduced in such a linear model. Supposing these coefficients are mutually independent, the covariance of the model error is derived by prescribing the variance of each coefficient as a function of wavenumber and wave type (Dee, 1990). However, this theory applies strictly only to linear dynamics, which is not a realistic situation.

We preferred a diagonal form to a non-banded one for the following two reasons: (a) the computational demands are far greater for non-banded forms; (b) optimality in the choice of a non-banded form is not warranted when nonlinear input functions and parameters are involved. Thus, more complex formulation will not necessarily produce better results (Lee and Georgakakos, 1996). Fortunately, a diagonal form has been found to yield good estimates for a number of practical applications (Lee and Georgakakos, 1996; French et al., 1994). Because of its operationality, we assume that the covariance error matrix $\mathbf{Q}_k$ is diagonal for practical purposes. As with the observational error, the prediction error is assumed proportional to α. Each diagonal element $\mathbf{q}_k$ of $\mathbf{Q}_k$ can be expressed as

$$\mathbf{q}_k = (\alpha_k^{\mathrm{f}} \cdot \gamma)^2, \tag{35}$$

where γ is the coefficient that indexes the model prediction error.

4. Application to rainfall prediction

As an application, we used data from a C-band volume scanning radar, called the Miyama radar, which is operated by the Ministry of Construction of Japan. The wavelength is 5 cm. The average resolution is about 3 km by 3 km horizontally, 1 km vertically, and 5 min temporally. The quantitatively observable radius is about 120 km. Nakakita et al. (1990, 1991) described the characteristics of this radar in more detail. A utilization of GPV data and AMeDAS for estimating the meso-α moisture field is presented in Nakakita et al. (1996).

All variables are defined at the same s levels in the vertical. For instance, radar data are transformed to Cartesian coordinates by combining segments of the various scans. This technique is well known as the Constant Altitude Plan Position Indicator (CAPPI). All required values from GPV data are transformed into the same Cartesian coordinates by an interpolation using Legendre's transformation, which produces a distribution smoother than that from the linear interpolation. Vertical levels are defined as $s = 0$, 1/1100, 1/220, 1/110, 2/110, 4/110, 6/110, 8/110, 10/110, 12/110, 15/110, 20/110, 30/110, …, 80/110, 90/110, 100/

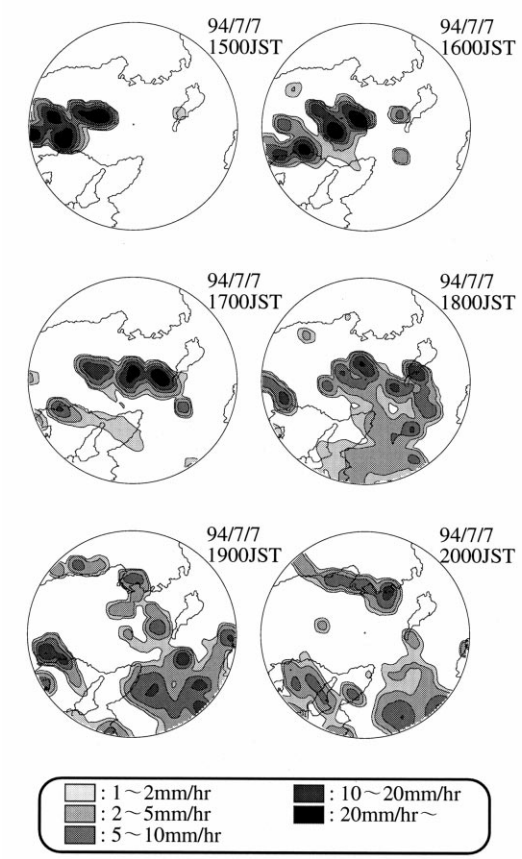

Fig. 4. Hourly sequential rainfall distributions from 1500 hrs JST, July 7, 1994, to 2000 hrs JST, July 7, 1994.

110, and 110/110. If the terrain height is zero, these correspond to elevations of 0, 10, 50, 100, 200, 400, 600, 800, 1000, 1200, 1500, 2000, 3000, …, 8000, 9000, 10 000, and 11 000 m above the surface, respectively. All basic equations are approximated by finite difference equations with the forward scheme for temporal terms, the upstream scheme for advective terms, and the central differential scheme for all the other terms. The horizontal grid spacing is 9 km over the region of interest, and the temporal increment of the finite difference is 15 s.

The test area is the one used previously by Nakakita et al. (1996, Fig. 5) for their deterministic method. The model domain spans 450 km in the east–west direction and 585 km in the north–south direction, with a center at longitude 135°22′W and latitude 35°02′N. The radar is located at the center of the model domain. The terrain is very complex in the southeast and west–northwest region of the radar observation area (Fig. 3).

The prediction method is applied to a rainfall event of July 7, 1994, which occurred along a stationary front during the Baiu rainy season. Fig. 4 shows the sequence of observed rainfall distribution for the height of 3.5 km from 1500 to 2000 hrs Japan standard time (JST). Rainfall intensity is computed by the moving average to a resolution of 15 km by 15 km (horizontally) and 20 min (temporally). The rainfall area is expanding under the influence of the complex terrain; it is difficult to predict using only simple advection of the rainfall distribution.

Two parameters that are the indices of error variances are determined manually by trial and error. The parameter spaces of the corresponding coefficients are defined by the range of γ over [0.1,3.0] and the range of σ over [0.1,1.0] with 0.1 resolution. The stochastic predictions, which are valid for 4 h in advance, are done offline for each pair of coefficients, and the predicted results are measured using performance criteria defined later. The predictions are started at 1-h intervals from 1500 hrs JST to 2100 hrs JST. For overall predictions, the optimal pair of coefficients is searched.

We determined that γ equals 0.3 and σ equals to 0.6 for this application. These show that the model was accurate within plus or minus 30% and that recursive observations were available with accuracy within plus or minus 60%. The value of σ implies that the estimated mixing ratio of the precipitation particles would be good data on the basis of the 40% criterion given in Georgakakos and Krajewski (1991); this assumes that recursive observations include the intermediate variable m_1^* predicted in the procedure of rainfall prediction.

4.1. Results of prediction

The predictions by this physically based stochastic method are compared with predictions using a persistence method and also with predictions using an advection method. Persistence means that the latest available radar observation is equal to the prediction without growth, decay, and advection of the rainfall field. The advection technique used in this study assumes a linear vector as proposed by Takasao and

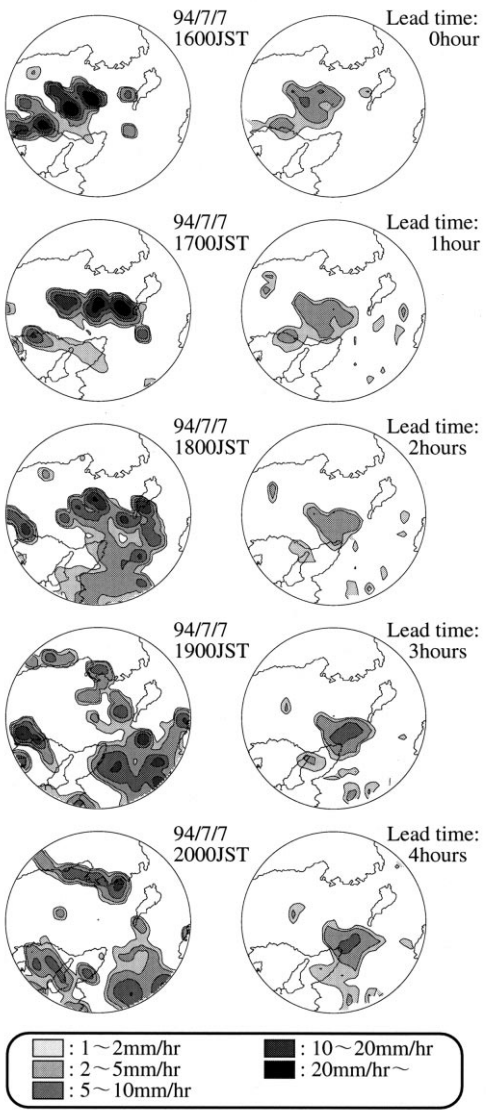

Fig. 5. Radar-observed and predicted rainfall distributions in hourly intervals using the deterministic method. The prediction is valid up to 4 h in advance.

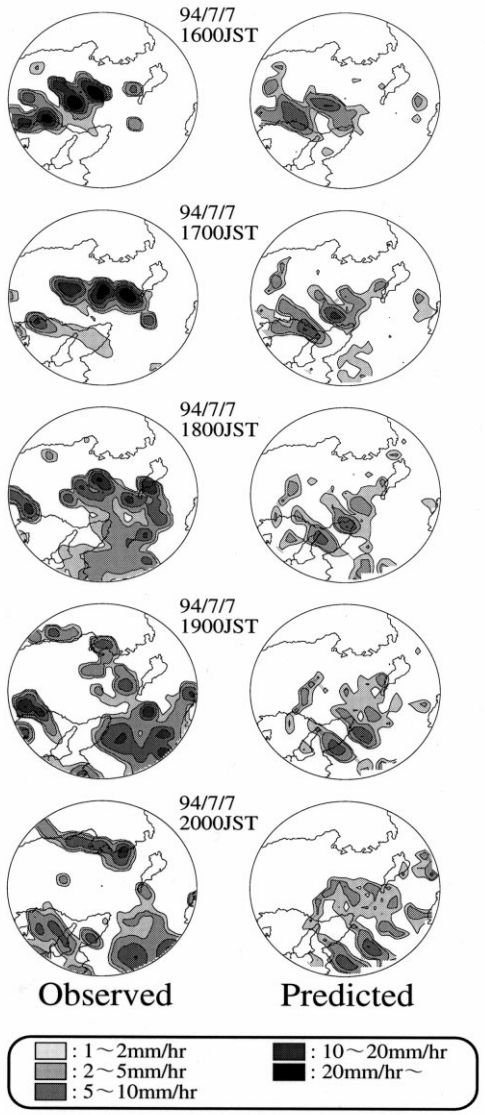

Fig. 6. Radar-observed and predicted rainfall distributions in hourly intervals using the stochastic method. The prediction is valid up to 4 h in advance.

Shiiba (1985). The prediction was calculated by extrapolating the latest radar data along the estimated vector without growth and decay of the rainfall intensity.

Figs. 5 and 6 provide radar-observed and predicted rainfall distributions from 1600 hrs JST, July 7, 1994, to 2000 hrs JST, at 1-h intervals for the height of 3.5 km. The left-hand and right-hand columns show the radar-observed distributions and the predicted results, respectively. The predictions are valid up to 4 h in advance. Fig. 5 shows the result predicted by the deterministic method. The starting time of prediction is 1600 hrs JST, July 7, 1994. Fig. 6 shows the result using the stochastic method. The starting time of this prediction is 1500 hrs JST because the prediction in Fig. 6 is based on the model parameter updated at 1500 hrs JST and 1600 hrs JST.

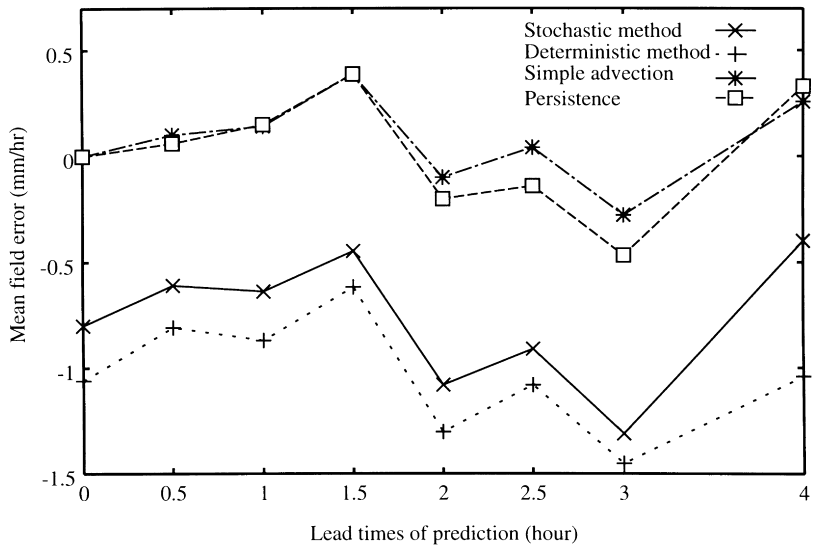

Fig. 7. Error in rainfall rate for the July 7, 1994 event.

It can be seen that the rainfall distributions predicted by the stochastic method are a better match to the observed patterns than are those predicted by the deterministic method. Fig. 6 shows further improvement in predicting rainfall areas that expand as they pass over mountainous regions. Figs. 7–9 show the performance scores for prediction times up to 4 h in advance from the stochastic method, the deterministic method, the persistence, and the advection method. Performance criteria used for the comparison include the domain-averaged mean error BIAS in rainfall rate shown in Fig. 7, root mean square error (RMSE) in Fig. 8, and a domain average cross-correlation coefficient (CC) in Fig. 9 between predictions and corresponding observations of rainfall intensities. Because the radar data are important input

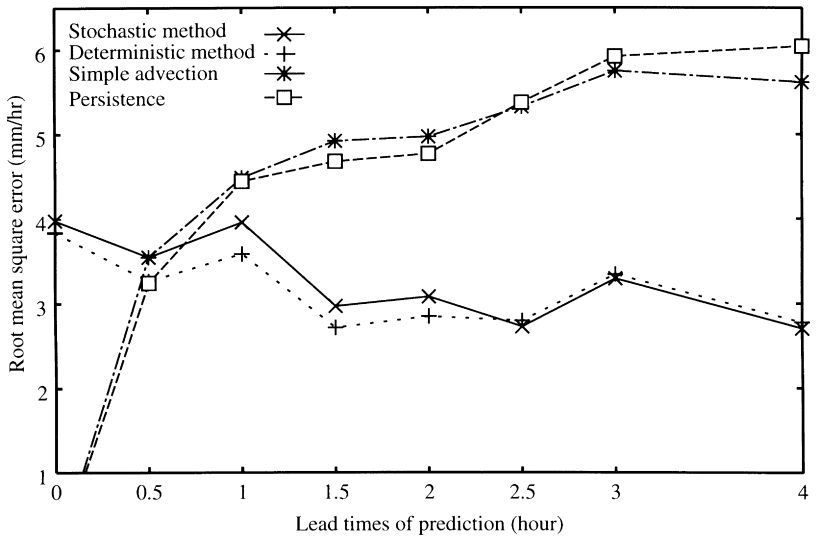

Fig. 8. Root mean square error in rainfall rate for the July 7, 1994 event.

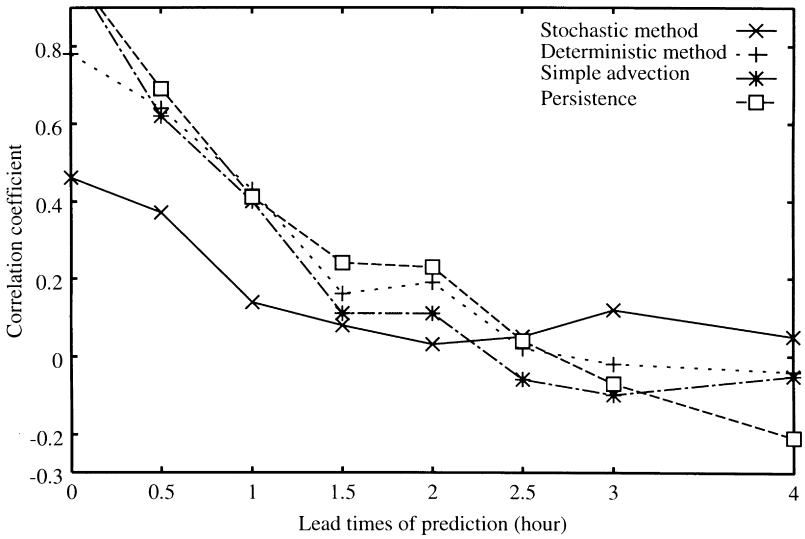

Fig. 9. Correlation coefficient for the July 7, 1994 event.

to the prediction method, predictions for locations in areas where advection would have come from outside the radar coverage should be evaluated separately. Therefore, only the downwind half of the radar field is evaluated so that the benefit of the added radar data or the performance of the method can be estimated. Note that the performances at 3.5-h lead time are not evaluated because the radar data are missing.

In most cases, both the advection and the persistence methods work as well as or better than other methods for the 1-h predictions. The predictions by the physically based method show good skill for lead times longer than 1 h. This indicates that the persistence and the advection methods are useful only when a rainfall event is stationary and characterized by negligible growth and decay over the prediction times. Though a larger BIAS of the physically based method implies that predicted rainfall amounts are underestimated due to the underestimation of the CRWV (Nakakita et al., 1996), usefulness of the conceptual rainfall model is reflected in smaller RMSE and higher CC. The stochastic method improves this underestimation problem, which leads to a BIAS of the stochastic method smaller than that of the deterministic method. Additionally, the stochastic method performs better than the deterministic method and produces a slightly higher CC and a slightly smaller RMSE for lead times longer than 2.5 h. These results indicate that newly observed and forecasted data can be utilized effectively within the stochastic framework.

Figs. 10 and 11 show the distributions of the model

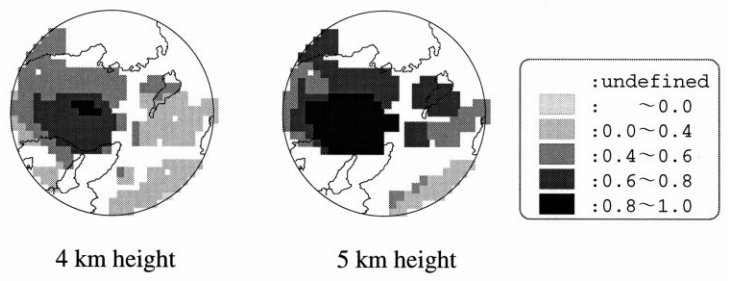

Fig. 10. A priori distributions of the model parameter for the heights of 4 and 5 km at 1500 hrs JST, July 7, 1994.

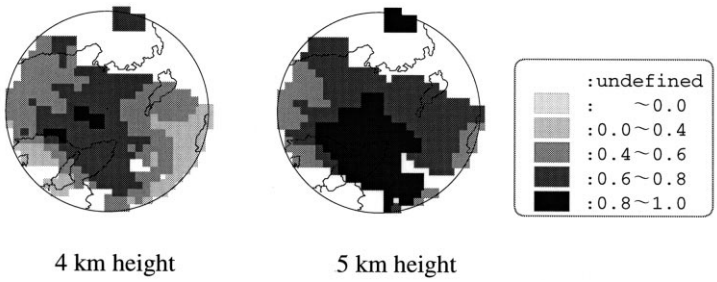

Fig. 11. A posteriori distributions of the model parameter for the heights of 4 and 5 km at 1600 hrs JST, July 7, 1994.

parameter for the heights of 4 and 5 km. The a priori fields of the model parameter shown in Fig. 10 are updated to the a posteriori fields shown in Fig. 11 to lessen the underestimation of the localized high rainfall amounts.

Figs. 12 and 13 provide radar-observed (left-hand column) and predicted (right-hand column) rainfall distributions. These differ from Figs. 5 and 6 in that the predictions in Figs. 12 and 13 are valid for 1-h in advance. So, prediction times longer than 1 h are not used as information for the update process. Figs. 12 and 13 show the results from using the deterministic method and the stochastic method, respectively. The images predicted by the stochastic method more closely match the intense rainfall patterns. In the deterministic method, the model state is reinitialized using each time observation and stochastic elements associated with uncertainties are ignored. These results indicate that utilizing GPV data with low accuracy of forecasts is likely to decrease the performance of rainfall prediction and that the stochastic framework reduces the instability of performance in the deterministic model.

As a result of the above application, improved model behavior is observed when the stochastic method is used. The deterministic method is extended to the stochastic method more suitable for real-time prediction. The weaknesses of this stochastic framework are identified as future research themes in Section 5.

4.2. Discussion

We now describe on uncertainties of radar-rainfall estimates. The estimates of the radar-based rainfall intensity r and the mixing ratio of precipitation particles m_l involve some uncertainties known such as ground clutter and the bright-band (melting layer). Regarding uncertainty problems, Battan's text (1973) and Doviak and Zrnić (1993) are good sources of information.

In this work, the radar data are corrected for ground clutter by the moving target indicator (MTI). Thus, angles below 1.0° can be selected as the lowest beam angle, even over the mountainous terrain. This situation makes it possible to detect rainfall produced by relatively low-level clouds. In the case of the radar used in this work, the lowest elevation angle was set at 0.4° and the height of the circular cylinder's bottom was about 1.5 km. The melting layer was at a height of about 4.5 km in the rain event studied here. Therefore, we compared the predicted results with the observed radar data at the height of 3.5 km, which is below the bright-band.

Distinguishing ice from liquid phases of precipitation is a long-standing problem in radar meteorology. In fact, radar techniques have practical limitations and their accuracy in rainfall estimation is highly suspect. However, radar has a significant advantage in that it can survey wide areas and make millions of measurements in minutes (Doviak and Zrnić, 1993). Georgakakos and Krajewski (1991) demonstrates by their covariance analysis together with Georgakakos and Bras model (1984a) that radar data are valuable for estimating vertically integrated liquid water content.

In this work, an operational procedure based on Nakakita et al. (1991, 1996) was used to take into account the uncertainties mainly due to the bright-band. Their procedure produces a smoothed vertical profile of both r and m_l by reducing, as much as possible, the gap between the estimated values of the grid points above and below the 0°C layer (i.e.

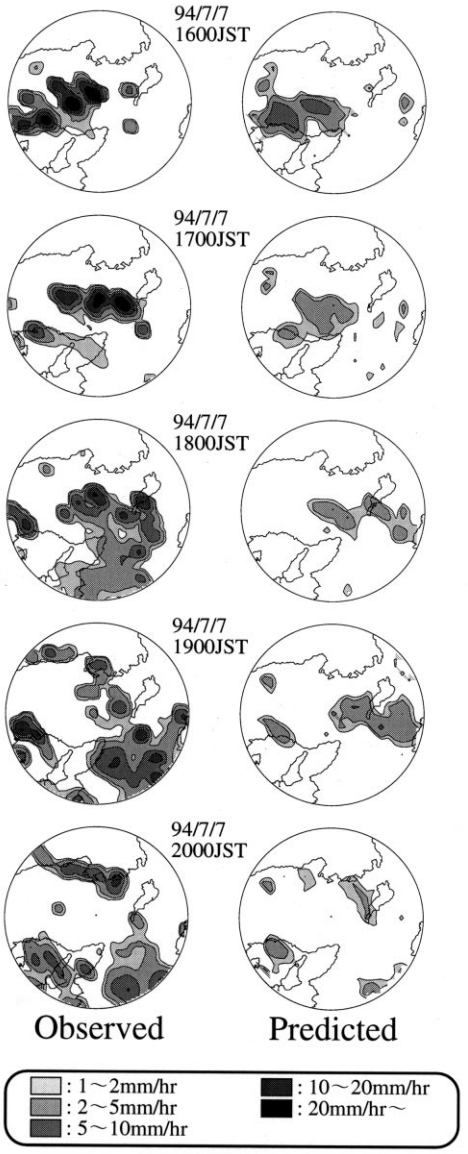

Fig. 12. Radar-observed and predicted rainfall distributions in hourly intervals using the deterministic method. The prediction is valid for 1 h in advance.

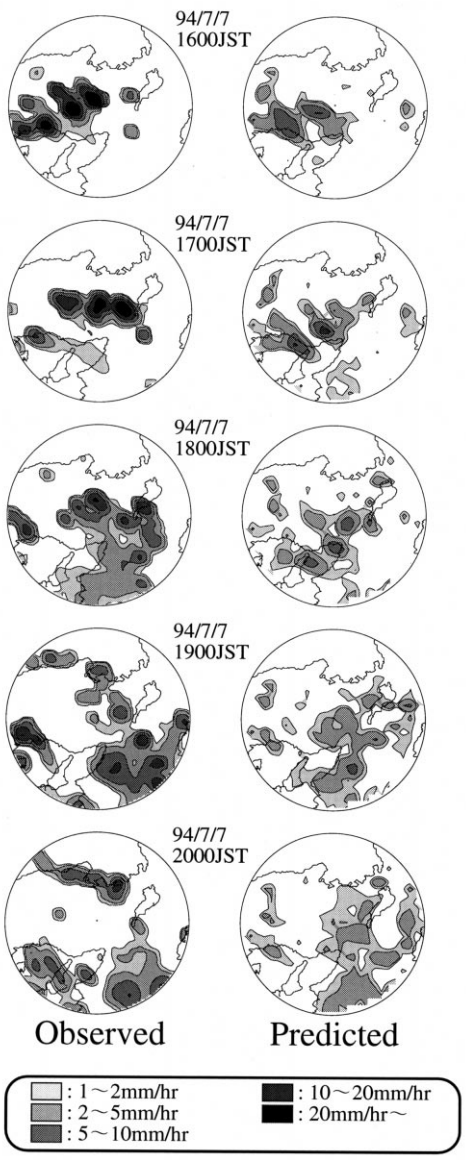

Fig. 13. Radar-observed and predicted rainfall distributions in hourly intervals using the stochastic method. The prediction is valid for 1 h in advance.

the bright-band of stratiform clouds). This procedure plays a crucial role in retrieving the CRWV with accuracy using Eq. (1) because the sensitivity analysis investigated by Nakakita et al. (1991) demonstrates that the CRWV is the most sensitive to the vertical gradient of r. Nakakita et al. (1996) provides a detailed and fruitful discussion on the applicability of this procedure.

5. Conclusions and future research directions

A stochastic rainfall prediction method has been formulated and evaluated. The method presented and tested herein is an extension of the deterministic method developed by Nakakita et al. (1996). This work presents a state–space mathematical model

that uses the extended Kalman filter and evaluates the model using several performance indices to quantify the behavior of the method.

The performance of the stochastic method is compared with that of the determinstic method, the persistence, and an advection method. The results of rainfall prediction produced by the stochastic method were more accurate than other methods for lead times longer than 2 h. This indicates that the stochastic method can effectively use newly observed radar data and forecasted GPV data, and also that the stochastic method is more suitable for real-time prediction.

Further research on this method is needed in the following three areas. With regard to the stochastic framework, calibration of the filter parameters, which represent observation and model errors, require more investigation. These parameters were calibrated manually by trial and error in this work. However, these parameters should be considered automatically with data observed in the past and predicted results in advance. A sensitivity analysis should be also conducted to clarify the dependence of the formulated stochastic rainfall prediction method on these parameters.

As an alternative approach, adaptive algorithms for estimating error covariances, both of the model and the observations, could be applied. Dee et al. (1985) has shown that the covariances can be estimated during the course of data assimilation without undue increase in computational burden. Another interesting study is Rajaram and Georgakakos (1989), which developed a physically based parameterization of the elements of the covariance matrices using only two parameters.

Second, the stochastic framework could be extended by including statistical estimation (Gelb, 1974) as a nonlinear filter. Generally speaking, such an estimation is more accurate than the Taylor expansion method. In this work, we have demonstrated that the stochastic concept improves the performance of rainfall prediction. Hence, utilization of new data might be more effective if some statistical estimation method is applied to the data.

Third, the rainfall prediction method is inadequate for simulating and predicting high rainfall intensities from convective rainfall events that are affected by smaller-scale updrafts or downdrafts. In fact, the model parameter is useful for modeling the shortage of the vertical flux of water vapor. Underestimated water vapor is not, however, compensated by an additional vertical wind motion. Nakakita et al. (1996) suggested that the CRWV could be underestimated mainly because of the underestimated vertical motion. This view is related to the known limitation that the wind field obtained from GPV data does not have sufficient spatial resolution to resolve convective processes on meso-β or meso-γ scales. In this sense, our proposed rainfall prediction method requires the improved performance from NWP, which is common with other methods that use a conceptual rainfall model.

In parallel with this work, Nakakita et al. (1998b) has presented a new conceptual rainfall model that parameterizes the vertical transport of water vapor in terms of CAPE and attempted to introduce this concept into the deterministic method. Nakakita et al. (1998c) has also proposed a method of estimating the updraft velocity at the meso-β scale using conventional radar. It is important that these other methods should be combined with our method, so that our stochastic conceptual model can utilize the updraft velocity at the meso-β scale.

Acknowledgements

The authors are grateful to the Yodo River Dams Control Office of the Ministry of Construction of Japan for providing the radar data used in this study. We also thank the anonymous reviewers for their suggestions and comments, which led to the improvement of the paper.

Appendix A. Integration procedure of the governing equations

Given the initial wind field and boundary conditions of the area of interest, it is possible to integrate the governing equations and determine the three-dimensional distribution of water at each time step. The integration of the conservation equations (1)–(3) is done in two steps in a manner similar to the method presented by Asai (1965) and used by Soong and Ogura (1973) and Colton (1976).

First, we calculate intermediate values of θ^*, m_v^*,

and m_l^* at the next step using only the dynamic terms in the equations. If $m_v^* > (1-\alpha)m_s^*$, condensation must occur to keep the air from becoming supersaturated. Letting

$$\delta m^{**} = m_v^* - (1-\alpha)m_s^*, \tag{A1}$$

and assuming that the process is isobaric, the amount of vapor to condense can be derived (see Ogura and Takahashi (1973)) as

$$\delta m = \delta m^{**}\left[1 + \frac{(1-\alpha)m_s^*}{\theta^{*2}}\frac{L^2}{C_p R_v}\left(\frac{1000}{p}\right)^{2R_d/C_p}\right]^{-1}, \tag{A2}$$

where R_v is the gas constant for water vapor and α the model parameter at the current time. A similar representation is used if $m_v^* < m_s^*$ and $m_l^* > 0$ (i.e. the evaporation condition is met). The maximum possible condensation or evaporation should be m_v^* or m_l^*, respectively.

The final predicted values of θ, m_v, and m_l at the next step are then

$$\theta = \theta^* + \frac{L}{C_p}\left(\frac{1000}{p}\right)^{R_d/C_p}\delta m, \tag{A3}$$

$$m_v = m_v^* - \delta m, \tag{A4}$$

$$m_l = m_l^* + \delta m. \tag{A5}$$

If neither the condensation condition nor the evaporation condition is met, the values of θ^*, m_v^*, and m_l^* become the predicted values of θ, m_v, and m_l with no additional adjustments.

References

Anderson, B.D.O., Moore, J.B., 1979. Optimal Filtering. Prentice-Hall, Englewood Cliffs, NJ.

Andrieu, H., French, M.N., Thauvin, V., Krajewski, W.F., 1996. Adaptation and application of a quantitative rainfall forecasting model in a mountainous region. J. Hydrol. 184, 243–259.

Asai, T., 1965. A numerical study of air–mass transformation over the Japan Sea in winter. J. Meteorol. Soc. Jpn. 43, 1–15.

Austin, G.L., Bellon, A., 1974. The use of digital weather records for short-term precipitation forecasting. Q. J. R. Meteorol. Soc. 100, 658–664.

Battan, L.J., 1973. Radar Observation of Atmosphere. University of Chicago Press, Chicago, IL.

Bellon, A., Austin, G.L., 1978. The evaluation of two years of real-time operation of a short-term precipitation forecasting procedure (SHARP). J. Appl. Meteor. 17, 1778–1787.

Bellon, A., Zawadzki, I., 1994. Forecasting of hourly accumulations of precipitation by optimal extrapolation of radar maps. J. Hydrol. 157, 211–233.

Bennett, A.F., Budgell, W.P., 1987. Ocean data assimilation and the Kalman filter: spatial regularity. J. Phys. Oceanogr. 17, 1583–1601.

Bradlay, M.M., 1984. The numerical simulation of orographic storms. PhD thesis, University of Illinois.

Browning, K.A., Collier, C.G., 1989. Nowcasting of precipitation systems. Rev. Geophys. 27 (3), 658–664.

Cohn, S.E., Parrish, D.F., 1991. The behavior of forecast error covariances for a Kalman filter in two dimensions. Mon. Wea. Rev. 119, 1757–1785.

Colton, D.E., 1976. Numerical simulation of the orographically induced precipitation distribution for use in hydrologic analysis. J. Appl. Meteor. 15, 1241–1251.

Dee, D.P., 1990. Simplification of the Kalman filter for meteorological data assimilation. Q. J. R. Meteorol. Soc. 117, 365–384.

Dee, D.P., Cohn, S.E., Dalcher, A., Ghil, M., 1985. An efficient algorithm for estimating noise covariances in distributed systems. IEEE Trans. Automat. Control AC-30, 1057–1065.

Doviak, R.J., Zrnić, D.S., 1993. Doppler Radar and Weather Observation. 2nd Ed. Academic Press, San Diego, CA.

French, M.N., Krajewski, W.F., 1994. A model for real-time quantitative rainfall forecasting using remote sensing. 1. Formulation. Water Resour. Res. 30 (4), 1075–1083.

French, M.N., Andrieu, H., Krajewski, W.F., 1994. A model for real-time quantitative rainfall forecasting using remote sensing. 2. Case studies. Water Resour. Res. 30 (4), 1085–1097.

Gelb, A., 1974. Applied Optimal Estimation. The MIT Press, Cambridge, MA.

Georgakakos, K.P., Bras, R.L., 1984a. A hydrologically useful station precipitation model. I. Formulation. Water Resour. Res. 20 (11), 1585–1596.

Georgakakos, K.P., Bras, R.L., 1984b. A hydrologically useful station precipitation model. II. Applications. Water Resour. Res. 20 (11), 1597–1610.

Georgakakos, K.P., Hudlow, M.D., 1984. Quantitative precipitation forecast techniques for use in hydrologic forecasting. Bull. Am. Meteorol. Soc. 65, 1186–1200.

Georgakakos, K.P., Kavvas, M.L., 1987. Precipitation analysis, modeling, and prediction in hydrology. Rev. Geophys. 25 (3), 163–178.

Georgakakos, K.P., Krajewski, W.F., 1991. Worth of radar data in the real-time prediction of mean areal rainfall by nonadvective physically based models. Water Resour. Res. 27 (2), 185–197.

Gunn, K.L.S., Marshall, J.S., 1958. The distribution with size of aggregate snow flakes. J. Meteorol. 15, 452–466.

Jazwinski, A.H., 1970. Stochastic Processes and Filtering Theory. Academic Press, New York, NY.

Kalman, R.E., 1960. A new approach to linear filtering and prediction problems. Am. Soc. Mech. Eng. J. Basic Eng. 82D, 35–45.

LeDimet, F.-X., Talagrand, O., 1986. Variational algorithms for

analysis and assimilation of meteorological observations: theoretical aspects. Tellus 38A, 97–110.

Lee, T.H., Georgakakos, K.P., 1990. A two-dimensional stochastic–dynamical quantitative precipitation forecasting model. J. Geophys. Res. 95, 2113–2126.

Lee, T.H., Georgakakos, K.P., 1996. Operational rainfall prediction on meso-γ scales for hydrologic applications. Water Resour. Res. 32 (4), 987–1003.

Marshall, J.S., Palmer, W.M.K., 1948. The distribution of raindrops with size. J. Meteorol. 5, 186–192.

Nakakita, E., Shiiba, M., Ikebuchi, S., Takasao, T., 1990. Advanced use into rainfall prediction of three-dimensionally scanning radar. Stochastic Hydrol. Hydraul. 4, 135–150.

Nakakita, E., Shiiba, M., Ikebuchi, S., Takasao, T., 1991. Advanced use into rainfall prediction of three-dimensionally scanning radar. In: Clukie, I.C., Collier, C.G. (Eds.). Hydrological Applications of Weather Radar. Ellis Horwood, London, pp. 391–408.

Nakakita, E., Ikebuchi, S., Nakamura, T., Kanmuri, M., Okuda, M., Yamaji, A., Takasao, T., 1996. Short-term rainfall prediction method using a volume scanning radar and grid point value data from numerical weather prediction. J. Geophys. Res. 101, 26181–26197.

Nakakita, E., Ikebuchi, S., Sawada, N., Shiiba, M., Takasao, T., 1998a. A short-term rainfall prediction method using reflectivity detected by three-dimensionally scanning radar. In: Shepherd, G.W., Verworn, H.-R. (Eds.). Advances in Hydrological Applications of Weather Radar. SUG-Verlagsgesellschaft, Hannover, Germany, pp. 337–346.

Nakakita, E., Fujii, T., Miyake, K., Yamaji, A., Ikebuchi, S., 1998b. A study on a short-term rainfall prediction method based on a conceptual model (LFC MODEL) representing vertical transport of water vapor (in Japanese, with English Abst.). Ann. Disaster Prev. Res. Inst. Kyoto Univ. 41-B-2, 155–170.

Nakakita, E., Ikebuchi, S., Tanaka, M., Shiiba, M., Takasao, T., 1998c. Estimation of three-dimensional wind velocity and conversion rate of water vapor using reflectivity detected by three-dimensionally scanning radar. In: Shepherd, G.W., Verworn, H.-R. (Eds.). Advances in Hydrological Applications of Weather Radar. SUG-Verlagsgesellschaft, Hannover, Germany, pp. 222–232.

Ninomiya, K., Koga, H., Yamagishi, Y., Tatsumi, Y., 1984. Prediction experiment of extremely intense rainstorm by a very-fine mesh primitive equation model. J. Meteorol. Soc. Jpn. 63, 273–295.

Ogura, Y., Takahashi, T., 1971. Numerical simulation of the life cycle of a thunderstorm cell. Mon. Wea. Rev. 99, 895–911.

Ogura, Y., Takahashi, T., 1973. The development of warm rain in a cumulus model. J. Atmos. Sci. 30, 262–277.

Oriville, H.D., 1965. A numerical study of the initiation of cumulus clouds over the mountainous terrain. J. Atmos. Sci. 22, 684–699.

Phillips, N.A., 1982. A very simple application of Kalman filtering to meteorological data assimilation. Office Note 258, National Meteorological Center, Washington, DC.

Pielke, R.A., 1984. Mesoscale Meteorological Modeling. Academic Press, San Diego, CA.

Rajaram, H., Georgakakos, K.P., 1989. Recursive parameter estimation of hydrologic models. Water Resour. Res. 25 (2), 281–294.

Seo, D.J., Smith, J.A., 1992. Radar-based short-term rainfall prediction, . J. Hydrol. 131, 341–367.

Soong, S.T., Ogura, Y., 1973. A comparison between axisymmetric and slab-symmetric cumulus cloud models. J. Atmos. Sci. 30, 879–893.

Takasao, T., Shiiba, M., 1985. Development of techniques for online forecasting of rainfall and flood runoff. J. Nat. Disaster Sci. 6 (2), 83–112.

Wilk, K.E., Gray, K.C., 1970. Processing and analysis techniques used with the NSSL weather radar system. Radar Meteorol. Conf., vol. 14, pp. 369–374.

Yoshizaki, M., Ogura, Y., 1988. Two- and three-dimensional modeling studies of the Big Thompson storm. J. Atmos. Sci. 45, 3700–3722.